



Efficient synthesis of a new heterogeneous gold nanocatalyst stabilized by di-alkyne ligand and its applications for photocatalytic dye degradation and transfer hydrogenation reaction

Bhavesh Agrawal · Jinal Patel · Pranav Dave ·
Jaydev Thakarda · Tejveer Singh Anand ·
Prasenjit Maity

Received: 19 May 2020 / Accepted: 2 March 2021 / Published online: 6 March 2021

© The Author(s), under exclusive licence to Springer Nature B.V. 2021

Abstract A new form of carbon-based ligand supported robust heterogeneous gold nanocatalyst was synthesized and its potential catalytic applications are demonstrated. The high yield (> 90%) synthesis procedure involves ligand exchange between hydrophilic polyvinylpyrrolidone polymer stabilized gold nanoparticles (Au:PVP) with a di-alkyne ligand (1,4-Diethynylbenzene). The ultrasmall stabilized gold nanoparticles (1.8 ± 0.3 nm) are bonded to di-alkyne ligand through acetylenic carbon atom ($\equiv\text{C-Au}$) with an electronically conjugated 3D network. The synthesized material (Au-P1) was meticulously characterized using several spectroscopic and microscopic techniques, e.g., Fourier transform infrared spectroscopy (FTIR), optical absorption spectroscopy (UV-Vis), powder X-ray diffraction (PXRD), X-ray photoelectron spectroscopy (XPS), and transmission electron microscope (TEM) and thermogravimetric analysis (TGA). The Au nanocatalyst showed good photocatalytic activity for degradation of several organic dye molecules in aqueous phase under visible light irradiation in presence of oxidizing agent (H_2O_2). The proposed mechanism involves dye absorption on ligand surface through π - π interaction followed by transfer of electron from excited dye molecules to gold core through electronically conjugated ligand for generation of reactive oxygen species ($\cdot\text{OH}$). The catalyst has also been demonstrated for transfer

hydrogenation of organic carbonyl and nitro functional groups ($>\text{C=O}$, $-\text{NO}_2$) with potassium formate (HCOOK) as hydrogen source in water. The catalyst could be recovered by simple filtration, and it was reused up to five cycles for both of these catalytic transformations with complete retention of its catalytic activity.

Keywords 1,4-Diethynylbenzene · Gold nanoparticles · Heterogeneous catalyst · Photocatalysis · Electronic conjugation · Dye degradation

Introduction

Catalysis by gold nanoparticles has attracted considerable attention in recent years as evident from numerous reports on demonstration of a variety of heterogeneous (Hutchings and Haruta 2005), homogeneous (Zhu et al. 2010), and quasi-homogeneous (Tsukuda et al. 2011)-based gold nanocatalysts. A majority of these efforts have been directed toward aerobic oxidation of various organic functionalities by taking advantages of superior ability of gold nanoparticles for activation of molecular oxygen (Tsukuda et al. 2011; Yamazoe et al. 2014). In addition to that nanogold is capable to catalyze other important chemical transformations, e.g., hydrogenation (Corma and Serna 2006), transfer hydrogenation (Chavda et al. 2016), de-oxygenation (Ni et al. 2011), N-alkylation (He et al. 2010), carbon-carbon coupling reaction (Tsunoyama et al. 2004), and also in electrocatalytic transformations (Saqib and Halder 2018).

B. Agrawal · J. Patel · P. Dave · J. Thakarda · T. S. Anand ·
P. Maity (✉)
Institute of Research and Development, Gujarat Forensic Sciences
University, Gandhinagar 382007, India
e-mail: pmaity@gsfu.edu.in

Another important application by supported gold nanoparticle is degradation of organic dye in aqueous medium under photocatalytic condition (Arabatzis et al. 2003; Hussain et al. 2016; Depuccio et al. 2015; Trivedi et al. 2016; Wang et al. 2018; Xiong et al. 2010; Ren et al. 2015; Lu et al. 2011; Cheng et al. 2013; Bhowmik et al. 2015; Choudhary et al. 2017; Gupta et al. 2010).

The safe disposal and clean degradation of various industrial dye molecules generated from textile, cosmetic, paper, leather, pharmaceutical, and nutrition industries is a serious issue in present time (Lellis et al. 2019). These dye molecules can severely pollute aquatic environment with adverse effect on human health and aquatic life. The demand for highly active and reusable photocatalysts for clean photocatalytic degradation of various organic dye molecules is ever increasing due to increased environmental awareness. Various metal oxide semiconductor nanostructure-based heterogeneous photocatalysts have been tested so far for this purpose with major emphasis on TiO₂ (Akpan and Hameed 2009; Mishra et al. 2018). However, the majority of these semiconductor metal oxide-based photocatalysts absorb only in the UV region and thus leaving energy available in the visible region of the solar spectrum. In view of this limitation, a new class of photocatalysts has been developed with wide absorption characteristics spanning UV to visible region of the solar spectrum. Gold nanoparticle-based photocatalysts is gaining popularity in this direction due to its ability to absorb both UV and visible radiation, high activity, reusability, and easy synthetic procedures. The major categories of gold photocatalysts reported for dye degradation include metal oxide (TiO₂, ZnO, SiO₂, CuO, Fe₃O₄) supported Au NP (Arabatzis et al. 2003; Hussain et al. 2016; Depuccio et al. 2015; Trivedi et al. 2016; Wang et al. 2018), graphene material supported Au NP (Xiong et al. 2010; Ren et al. 2015; Lu et al. 2011), carbon nitride (C₃N₄) supported Au NP (Cheng et al. 2013; Bhowmik et al. 2015), and plant (leaf) extract stabilized Au NP (Choudhary et al. 2017; Gupta et al. 2010). The advantage of Au NP-based photocatalysis is that it can absorb a wide spectrum of light spanning UV to visible region. The surface plasmon resonance (SPR) effect is responsible for absorbing the visible region of light and the interband electronic transition from 5d to 6sp band absorb strongly in UV region (Sarina et al. 2013). However, due to high surface energy, Au nanoparticles tend to agglomerate in solution (colloidal) phase; hence solid material supported heterogeneous catalysts are preferred than quasi-

homogeneous colloidal gold catalysts from the view point of their robustness (higher stability) and easy catalyst separation for recycling. Apart from stability, the support material can also electronically influence the Au NP and tune its catalytic activity, thus leaving the role of support material very significant (Xiong et al. 2010; Ren et al. 2015). Graphene and reduced graphene oxide supported gold photocatalysts reported in recent times are showing very promising results due to strong electronic synergy between graphene and gold (Xiong et al. 2010; Ren et al. 2015; Lu et al. 2011). Here it is to be mentioned that Au NP only forms stable composite system on graphene surface through creation of carbon-vacancy defect and the functional groups present in the chemically derived graphene. In view of this, a suitable synthetically simple system mimicking graphene supported gold photocatalysts where gold is electronically conjugated to support will be very interesting. Electronically conjugated alkyne stabilized gold nanoparticles reported by us will be an ideal choice for this purpose due to strong electronic conjugation between metal and ligand and high stability of such systems (Maity et al. 2011, 2012, 2013; Srivastav et al. 2017; Yamamoto et al. 2017; Dave et al. 2019). However, metal nanoparticles stabilized by mono-alkyne ligands are nicely soluble in common solvents, and hence a new strategy is required to get conjugated polymer network of such ligand metal nanoparticle-based material as heterogeneous catalyst. This study reports the synthesis of a di-alkyne (1,4-Diethynylbenzene) stabilized polymeric gold nanocatalyst system and its efficiency for photocatalytic degradation of organic dye molecules under visible light irradiation.

On the other hand, catalytic transfer hydrogenation (TRH) of organic functional groups is an alternative way of hydrogenation under mild and safe conditions by using 2-propanol or formate as hydrogen source as opposed to the use of highly flammable molecular hydrogen under high pressure (Noyori and Hashiguchi 1997; Wang and Astruc 2015; Indra et al. 2013; Su et al. 2008; He et al. 2009). Despite tremendous effort has been put in utilizing nanogold for various catalytic transformations, its potential for TRH catalysis is very little explored. In recent years, Cao et al. have reported solid metal oxide (TiO₂, Fe₂O₃, Al₂O₃, CeO₂) supported nanogold catalyzed TRH of carbonyl and nitro derivatives by using isopropanol and potassium formate as hydrogen source (Su et al. 2008; He et al. 2009). Their proposed mechanism involves the formation of bound hydride ions on CeO₂ surface followed by its transfer to

gold through reverse hydrogen spill over and then hydrogenation of carbonyl groups. Our recent work on polyvinylpyrrolidone stabilized quasi-homogeneous gold nanocatalyst (Au:PVP) for TRH catalysis showed good activity with the mechanism involving direct hydride formation on gold surface (Chavda et al. 2016). However, due to its quasi-homogeneous nature, catalyst recovery and recycling is little tedious. In view of this, an efficient heterogenous catalyst with good catalytic activity with ease of product and catalyst separation ability and long-time recycling ability will be appreciated. With this aim, the present study also demonstrates the application of synthesized gold nanocatalyst for transfer hydrogenation of carbonyl and nitro functional groups with special emphasis on its catalytic activity and reusability, and at the end a plausible reaction mechanism was also presented with the support of some experimental evidence.

Materials and methods

All starting materials and solvents were procured from commercial sources. 1,4-Diethynylbenzene, phenyl acetylene, styrene, hydrogen tetrachloroaurate tetrahydrate ($\text{HAuCl}_4 \cdot 4\text{H}_2\text{O}$), sodium tetrahydroborate (NaBH_4), polyvinylpyrrolidone, PVP (K30, 40 kDa), and hydrogen peroxide (30% aqueous solution) were obtained from Sigma-Aldrich Chemical Co. Carbonyl compounds, aromatic nitro compounds, aniline derivatives, alcohols, dye molecules, methylene blue (MB), rhodamine B (RhB), auramine (AUR), indigo-carmin (IN-CA), and Eosin Yellow (EY) were purchased from Finer Chemicals, India, and were used as received. Milli-Q grade water was used in all preparations, measurements, and as catalysis medium.

Optical absorption spectral measurements were carried out by using a JASCO V-670 spectrophotometer. FT-IR spectra were recorded by using a JASCO FT/IR-4200 spectrophotometer with samples prepared as KBr pellets. Transmission electron microscopic (TEM) images were recorded by using a Philips JEM 2000FX electron microscope operated at 200 kV equipped with an EDX detector. Field emission scanning electron microscopic (FE-SEM) image was captured by a Zeiss Supra 40VP FESEM operating with a 5 kV accelerating voltage. Powder X-ray diffraction (PXRD) pattern of Au-P1 catalyst was measured using X-ray diffractometer (GNR APD 2000 PRO) with a Cu-K α light source.

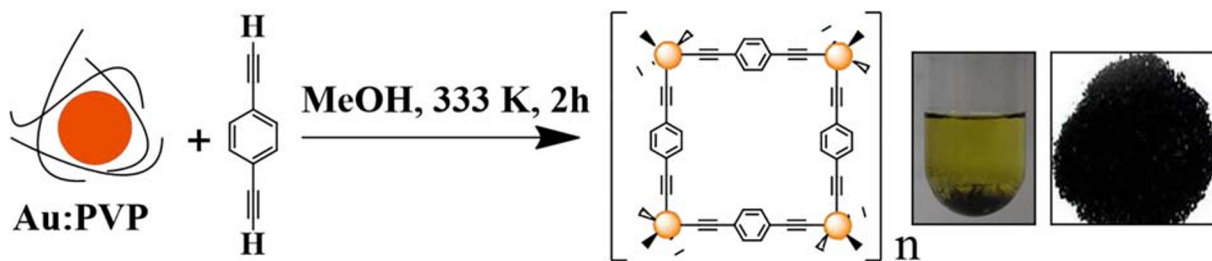
XPS measurement was performed on a JEOL, JPS-9010MC instrument (model no.-11120-0404) using Mg K α source. The catalyst was pressed to form pellet followed by vacuum drying before XPS measurement. The spectrum was calibrated with respect to C_{1s} peak which was adjusted at 285 eV value. Content of gold in the samples was determined on a Shimadzu plasma atomic emission spectrometer (ICPE-9000). Total organic carbon (TOC) of the aqueous dye solutions were determined by using a Shimadzu TOC equipment. Thermal gravimetric analysis (TGA) was carried out by using a Seiko TG/DTA 6300 analyzer under N₂ atmosphere with 1.6 mg samples. Electrospray ionization (ESI) mass spectra were recorded by using a micromass LCT instrument. The reaction yield for TRH reactions was determined by using a Shimadzu gas chromatograph (GC 14A) coupled with an FID detector and fitted with a silica capillary column (RTX-1).

Synthesis of the catalyst

PVP stabilized gold nanoparticle (Au:PVP) with 4 wt% metal content was synthesized and purified through lyophilization by following our previous protocol and used as precursor (Chavda et al. 2016). For the synthesis of Au-P1 catalyst, 500 mg of Au:PVP nanoparticle (1.26×10^{-3} mmol of Au) was dissolved in methanol (15 mL), and 0.5 g (4 mmol) 1,4-Diethynylbenzene was added to it under stirring condition at 333 K, and the reaction was continued for 2 h. The ligation of alkyne ligand to gold nanoparticles results in replacement of PVP ligand and formation of a 3D polymeric network of 1,4-Diethynylbenzene stabilized gold nanoparticles which precipitates out from the solution as a black material (Scheme 1). The reaction was cooled to room temperature; the product was filtered off and washed repeatedly with methanol followed by drying under vacuum to get final gold catalyst (Au-P1) with isolated yield of 142 mg (90 %) with respect to gold.

Photocatalytic dye degradation

All photocatalytic reactions were performed in a Pyrex glass photoreactor tube using a 200 W daylight lamp under stirring condition. Before irradiation of light, the dye solution (10 mL, 50 μM) and 5 mg of Au-P1 catalyst were kept under stirring for 30 min to allow the physical absorption equilibrium between dye molecules and the solid catalyst. Then 100 μL of H₂O₂



Scheme 1 Scheme showing synthesis of 1,4-Diethynylbenzene stabilized polymeric gold nanoparticle-ligand framework (Au-P1) along with the black precipitate of it during synthesis and after drying

solution was added, and the light source was switched on, and at specific time interval, the optical absorption value of the dye solution was measured using UV-Vis spectrophotometer. The catalyst from first batch of reaction was separated by filtration and washed repeatedly with water and acetone followed by drying at 60 °C for 6 h under vacuum. Then it was used for next batch of photocatalytic reaction with a model dye (MB) under above conditions. The recovery and reuse of the catalyst were performed up to five cycles in similar fashion.

Catalytic transfer hydrogenation of carbonyl and nitro compounds

The catalytic transfer hydrogenation reactions were performed in water by taking potassium formate as hydrogen source at 323 K. Substrate (0.5 mmol), Au-P1 catalyst (40 mg, 5 mol% Au with respect to substrate), and potassium formate (210 mg, 2.5 mmol) were added to 10 mL water in a 25 mL round bottom flask fitted with magnetic stirrer, heating mantle, and reflux condenser. The reaction was continued at 323 K for 8 h under stirring (600 rpm) to get the desired hydrogenation product. After completion of the reaction, the product was isolated through extraction with diethyl ether and then analyzed by GC and GC MS. The heterogeneous gold catalyst was recovered by filtration followed by washing with acetone and drying under vacuum before being reused for next cycle.

Results and discussion

Synthesis and characterization of the catalyst

1,4-Diethynylbenzene stabilized gold nanocatalyst (Au-P1) was synthesized via a ligand exchange strategy by taking Au:PVP nanoparticles as precursors using

methanol as solvent at 60 °C (Scheme 1) (Maity et al. 2011). Figure 1 shows the FTIR spectra of free ligand and Au-P1, TEM images, and absorption spectra of the Au-P1 and Au:PVP. The acetylenic $\equiv\text{C-H}$ stretching frequency present in the free ligand at 3290 cm^{-1} is completely absent in the Au-P1 indicating the breaking of acetylenic C-H bond followed by successful ligation of alkyne group to gold through C-Au bond (Scheme 1). We could also observe 100 cm^{-1} red shifted $\text{-C}\equiv\text{C-}$ stretching frequency in the Au-P1 as compared to free ligand where it is present at 2110 cm^{-1} due to weakening of the $\text{-C}\equiv\text{C-}$ bond through its electron transfer to gold. The carbonyl stretching frequency (1630 cm^{-1}) of Au:PVP (Fig. 1b) is totally absent in Au-P1, indicating its replacement by alkyne ligand. The TEM images (Fig. 1c,d and S1) of Au-P1 and its corresponding particle size histogram show uniform-sized particles with mean diameter of $1.8 \pm 0.3\text{ nm}$ as compared to $1.7 \pm 0.3\text{ nm}$ gold nanoparticles in the precursor Au:PVP, thus almost retaining the size of precursor gold particles. The FE-SEM image (Fig. S2) showed porous 3D structures of polymeric ligand-gold nanoparticle composite. Absorption spectra of the Au nanocatalyst features exponentially enhanced absorption band in the UV region due to interband $d \rightarrow sp$ electronic transition with no sign of plasmonic peak at 520 nm as evident from TEM analysis of small ($< 5\text{ nm}$) size of gold nanoparticles. The elemental composition and qualitative metal content were confirmed through energy dispersive X-ray spectroscopy (EDX) (Fig. S3), and as expected only the presence of carbon and gold was confirmed with approximate gold content of 16%. The quantitative metal content of the catalyst was determined by ICP-OES method, and we could find 12.8 wt% Au content in this material. This is to be mentioned that the metal content is quite high as compared to other supported gold nanocatalysts, but due to strong electronically conjugated 3d network of di-alkyne-based ligand frame, the

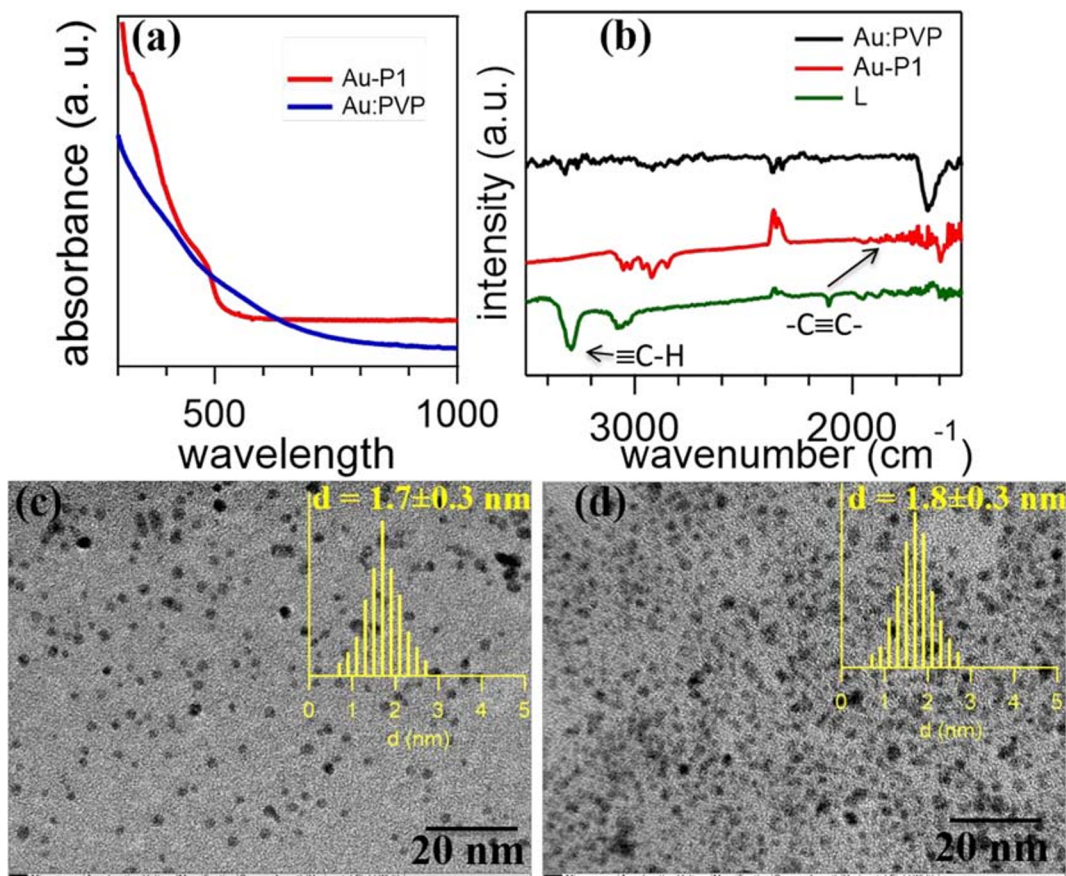


Fig. 1 **a** UV-Vis spectra of Au:PVP in aqueous solution and solid state absorption spectra of Au-P1, **b** FT-IR spectra of 1,4-Diethynylbenzene (L), Au:PVP, and Au-P1, **c** and **d** TEM image

with particle size distribution of Au:PVP and Au-P1 nanoparticles, respectively

system is very robust, and we could not find any agglomeration or leaching phenomenon as will be discussed in later part. The powder XRD profile of Au-P1 and Au:PVP (Fig. 2e) showed crystalline characteristics with three prominent peaks corresponding to (111), (220), and (311) crystalline planes of face-centered cubic (FCC) Au lattice (Sun et al. 2004). The chemical nature (oxidation state) of Au in the catalyst was determined by analyzing high-resolution (narrow scan) XPS spectra (Fig. 2a–c). A characteristic doublet peaks with binding energy values 83.8 eV and 87.8 eV were assigned for Au 4f_{7/2} and 4f_{5/2} orbital electrons, respectively, confirming the zero-oxidation state of Au (Leppelt et al. 2006). Thermogravimetric measurement of the Au-P1 (Fig. 2d) was also performed in the temperature range of 50 to 500 °C, which showed complete decomposition of organic moiety at 500 °C and a total wt. loss of 87.5%, thus leaving 12.5% metal content the system. Thus, the quantitative gold content in the

catalyst measured by ICP-OES (12.8%) and TGA analysis are in good agreement.

Photocatalytic degradation of organic dye molecules

The photocatalytic degradation of a total five different organic dye molecules (MB, RhB, AUR, IN-CA, and EY) were carried out in aqueous medium under visible light using Au-P1 catalyst, and the progress of those reactions was monitored by measuring absorption spectrum at different time intervals. We initially started with MB as a standard dye molecule for its photocatalytic degradation under varying conditions. Different control experiments were first carried out to fix the proper experimental parameters for degradation of MB. The absence of either light, oxygen, H₂O₂, or catalyst results no reduction of absorption value measured through UV-Vis spectra indicating that all are required for successful degradation of dye molecules. Next, the photocatalysis

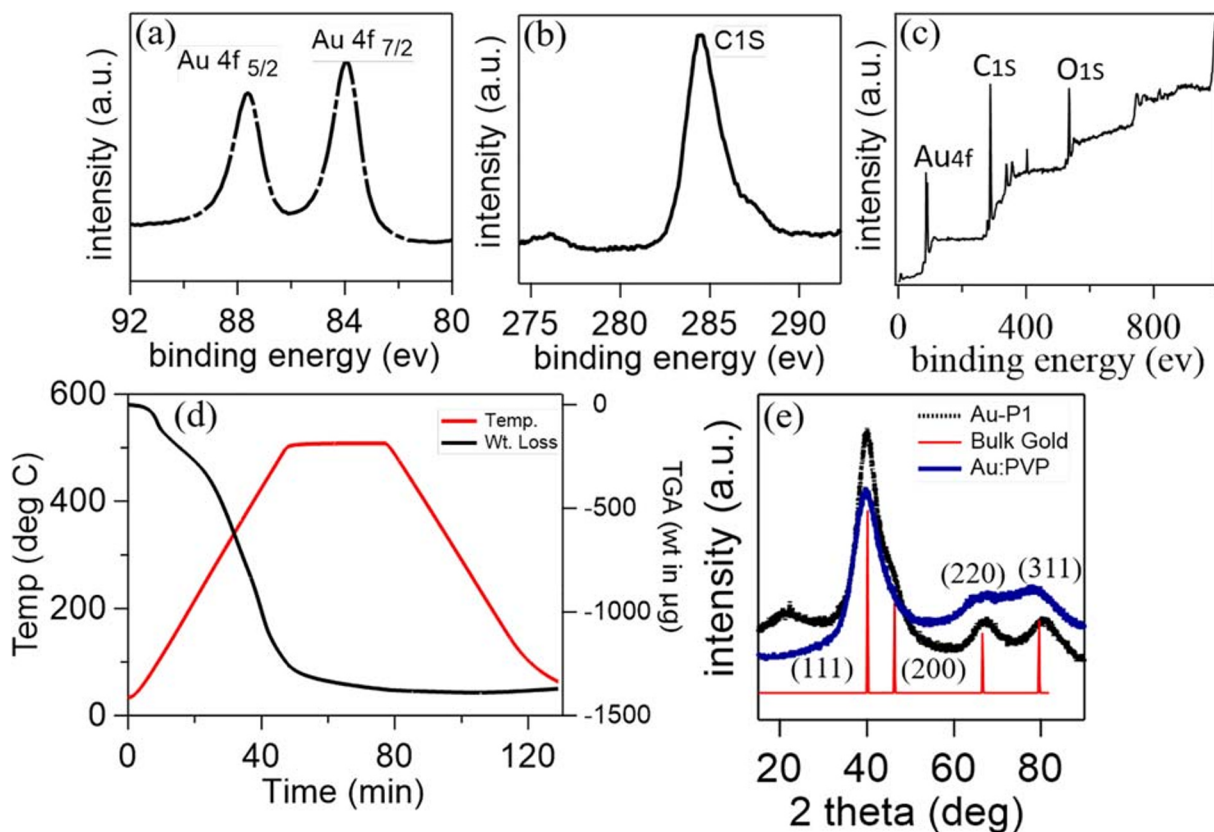


Fig. 2 XPS spectra of Au-P1 showing binding energy of (a) Au4f orbital electron, (b) C1s orbital electron and (c) wide scan XPS spectra of Au-P1, d TGA graph showing heat-induced degradation

profile of Au-P1, and e PXRD profile of the Au-P1 and Au:PVP nanopowders along with standard XRD pattern of bulk gold

experiment was performed by bubbling oxygen gas for a period of 30 min in presence of catalyst and under light irradiation while recording the UV-Vis spectra in every 5-min interval. The observed spectral profile (Fig. S4) shows very slow reaction with only 10% reduction of absorbance value. The use of hydrogen peroxide as oxidizing agent instead of molecular oxygen in next set of experiment results complete degradation of dye (MB) within 30 min time as evident from the UV-Vis spectra (Fig. 3a). After successful photocatalytic degradation of MB, we have tested the activity of the Au-P1 catalyst for photocatalytic degradation of other four organic dye molecules (e.g., RhB, AUR, IN-CA, and EY) under identical set of conditions using H_2O_2 as oxidizing agent for a period of 30 min, and the reaction was monitored in every 5 min (Fig. 3). As evident from the time monitored UV-Vis spectra, all experiments showed gradual decrease of optical absorption values indicating their significant photocatalytic decomposition. To evaluate the nature of the reaction, we have

calculated and plotted $\ln(A/A_0)$ versus time (Fig. 3f) for these five reactions which fits first-order kinetic model. The calculated rate constants for five dye compounds are as follows: MB, $8.9 \times 10^{-2} \text{ min}^{-1}$ ($R^2 = 0.9852$), RhB, $2.72 \times 10^{-2} \text{ min}^{-1}$ ($R^2 = 0.9481$), AUR, $2.49 \times 10^{-2} \text{ min}^{-1}$ ($R^2 = 0.9943$), IN-CA $3.98 \times 10^{-2} \text{ min}^{-1}$ ($R^2 = 0.9297$), EY $4.1 \times 10^{-2} \text{ min}^{-1}$ ($R^2 = 0.9728$).

However, decrease of specific absorption values cannot guarantee complete degradation of dye molecules, because it is possible that smaller fragmented molecules with different optical properties are generated rather than complete degradation of organic dye molecules. Hence full spectrum (wavelength range) of the UV-Vis profile of each dye molecule should be scrutinized to determine their complete degradation. As can be seen (Fig. 3a–e), we have measured the full spectrum of wavelength in the range of 200–800 nm for studying the extent of catalytic degradation of dye molecules. Mass spectrometric analysis of all dye solutions was also performed after photo treatment at two different

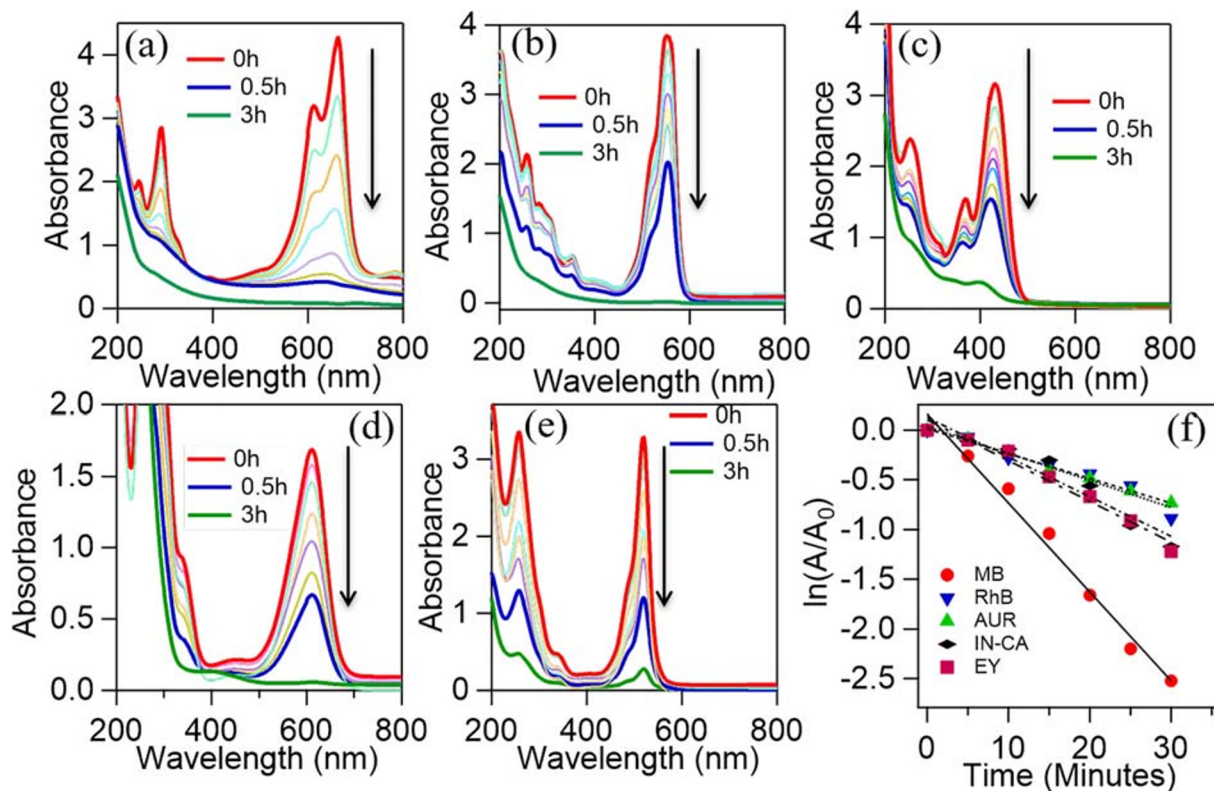


Fig. 3 a–e UV-Vis absorption spectra showing time monitored photodegradation of aqueous solutions of MB, RhB, AUR, IN-CA, and EY, respectively, by Au-P1 photocatalyst, f plotting $\ln(A/A_0)$ vs. time for these five dye compounds

time intervals (0.5 h and 3 h) to find out the traces of different degraded fragments (Fig. 4 and Fig. S5) under identical conditions. From the mass data measured after 30 min of dye degradation (Fig. 4), we could find the presence of molecular ion peaks and smaller fragmented peaks for all dye solutions except MB, indicating their incomplete degradation, which also corroborates with the UV-Vis absorption profiles (Fig. 3a–e). The fragmented molecular ion peaks obtained through this measurement are summarized in a table (Table S1). Through scrutiny of UV-Vis absorption profiles and mass data, it reveals that the extent of dye degradation follows the order MB > AUR ~ RhB > EY > IN-CA after 30 min of photocatalytic reaction. In continuation of this study, we have prolonged the photocatalytic reaction time up to 3 h and then again measured the corresponding UV-Vis spectra and mass spectral profiles (Fig. 3a–e and Fig. S5). The analysis shows completely diminished UV-Vis absorption profiles for all dye molecules and insignificant presence of peaks in the mass spectra indicating complete degradation of organic dye molecules. Further, to ensure the extent of

dye degradation, we have also determined the TOC values of dye solutions before and after photocatalysis experiments (Table S2). As mentioned earlier, it is well known that decolorization of dye does not guarantee its complete mineralization to CO_2 and H_2O . TOC values are better indicator to understand the extent of complete (clean) dye degradation, and as can be found for all the solutions, the TOC values are in single digit (< 10 ppm) after photocatalysis treatment.

The recycling ability of heterogeneous Au-P1 catalyst was also studied after filtration and drying of the catalyst in each successive catalytic run with MB as a standard dye. The activity was found to remain constant with more than 98% dye degradation for five successive catalytic cycles which were performed under identical conditions for a duration of 30 min and thus validates the robustness and its high catalytic activity (Fig. S6). TEM analysis of used catalysts showed monodispersed particles with mean diameter 1.9 ± 0.4 nm, hence confirming negligible agglomeration phenomenon (Fig. S7).

We have envisioned a possible reaction mechanism in view of the chemical structure and electronic

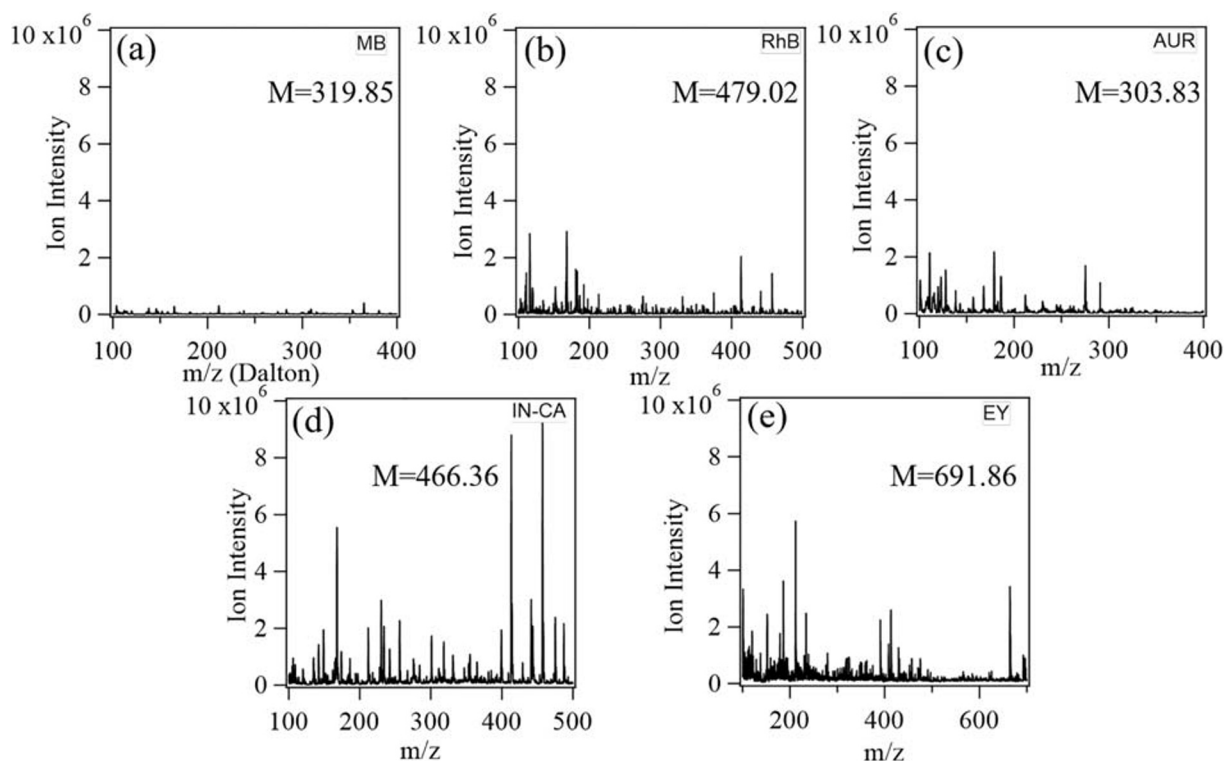


Fig. 4 ESI mass spectra of photodegraded (after 30 min) five different dye solutions (a) MB, (b) RhB, (c) AUR, (d) IN-CA, and (e) EY

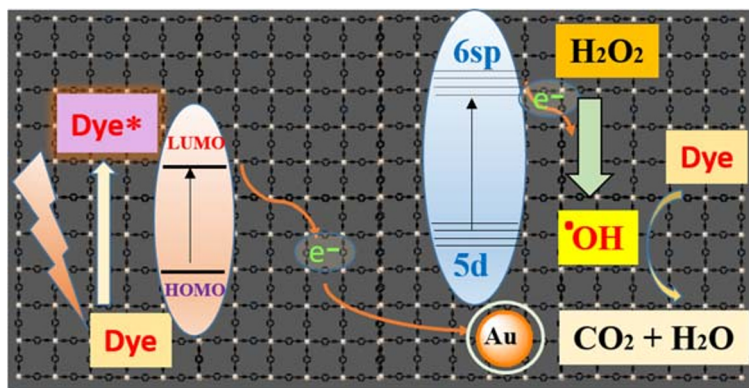
properties of Au-P1 catalyst, previous reported mechanism of supported gold photocatalysts (Xiong et al. 2010), and the obtained catalytic results in this study (Scheme 2). The presence of diethynylbenzene-conjugated units makes a pi electron-rich platform where organic dye molecules adsorb through π - π interaction thus initiates the first step. The close proximity of gold nanoparticles due to dialkyne framework may also ensure adsorbed dye molecules's direct interaction with gold. The photoexcitation of dye molecules (in visible region of spectrum) results electron transfer to gold core

through conjugated aromatic ligands. Afterwards, photoexcited electrons from 6sp band of Au generates highly reactive hydroxyl radical ($\cdot\text{OH}$) from H_2O_2 , which interacts and breaks down the dye molecules.

Transfer hydrogenation of carbonyl and nitro derivatives

After successful demonstration of photocatalytic activity of Au-P1 catalyst, its efficacy for transfer hydrogenation reaction was evaluated for selected organic

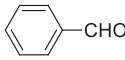
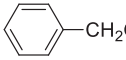
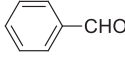
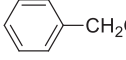
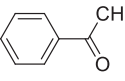
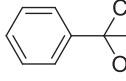
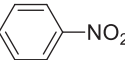
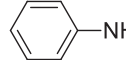
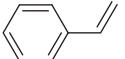
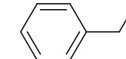
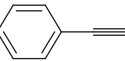
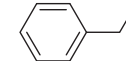
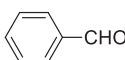
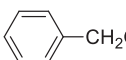
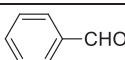
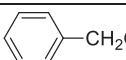
Scheme 2 Proposed mechanism of visible light induced photocatalytic degradation of organic dye by Au-P1 nanocatalyst.



functional groups (ketone, $>C=O$; aldehyde, $-CH=O$; Nitro, $-NO_2$; alkene, $-CH=CH_2$; and alkyne, $-C\equiv C-H$). The reactions were carried out in water by using potassium formate as hydrogen source at 323 K temperature for a duration of 8 h (Table 1). Benzaldehyde was taken as a standard substrate to optimize the reaction parameters. Initial blank tests were carefully carried out, and it was confirmed that the absence of catalyst or formate salt does not yield any desired product (Table 1, entry 1). The reaction of benzaldehyde with 5 mol% catalyst and 5 equivalent potassium formate at a temperature of 353 K for 8 h results complete conversion ($> 99\%$) to benzyl alcohol (Table 1, entry 1). Lowering the temperature to 323 K, while keeping other parameters the same, gives us a benzyl alcohol conversion of 86% (Table 1, entry 2), and afterward, this set of condition was taken as a standard for scrutinizing the efficacy of the catalyst for other substrates. The conversion of acetophenone (55%, entry 3), nitrobenzene (78%, entry 4), styrene ($< 1\%$, entry 5), and phenyl acetylene ($< 1\%$, entry 6) were observed under given set of conditions. The results show that the catalyst could efficiently

reduce carbonyl and nitro compounds but inactive against alkene and alkyne functional groups. The recycling ability of Au-P1 catalyst was also evaluated for benzaldehyde hydrogenation up to five cycles with equal conversion efficiencies even after five cycles (Table 1, entry 7). This is also to be mentioned that the catalyst was separated by simple filtration followed by washing with acetone and drying before being used for next cycle of reaction. The results so far discussed imply high catalytic activity, ease of catalyst separation for recycling, and efficient reusing capacity of the catalyst for transfer hydrogenation of carbonyl and nitro functional groups. Next, we tried to shed light on a plausible catalytic pathway for activation of formate ions on gold surface. There are two possible pathways (Gilkey and Xu 2016) for the activation of formate ion on gold surface to donate (transfer) its hydrogen to the substrate and subsequently produce hydrogenation product (Scheme S1). In the first pathway, formate ions first get adsorbed on gold surface along with substrate, and then gold-hydride (Au-H) intermediates are formed followed by transfer of hydride to substrate (*metal*

Table 1 Transfer hydrogenation of selected substrates catalyzed by Au-P1 in water^a

Entry	Substrate	Product	% Conversion
1			99 ^b (0 ^c , 0 ^d)
2			86
3			55
4			76
5			< 1
6			< 1
7			86 ^e , 84 ^f , 85 ^g , 80 ^h , 82 ⁱ
8			5 ^j

^a Au-P1 40 mg (5 μ mol Au), substrate 0.5 mmol, HCOOK 2.5 mmol, water 10 mL, temperature 323 K, time 8 h. ^b at 353 K; ^c same conditions, except addition of HCOOK, ^d same conditions, except addition of catalyst. ^{e,f,g,h,i} 1st, 2nd, 3rd, 4th, 5th recycle results. ^j Substrate added 8 h after formate addition and reaction continued for another 8 h

hydride route). In the alternate pathway, gold activates the adsorbed formate ion electronically and promotes direct transfer of hydride ion to substrate molecules without forming metal hydride intermediate (*direct hydride transfer*) (Scheme S1). Control experiments were carried out to find out the correct pathway of formate ion activation. It is understood that in the first pathway (*metal hydride route*), formate ions will decompose with time even in absence of substrate (aldehyde) through the formation of CO₂ and H₂ due to gold catalyzed activation process, whereas in the second pathway, formate ions could only be consumed if suitable substrates (carbonyl or nitro) are present in the reaction medium. Our control experiment showed that formate ions get decomposed by Au-P1 catalyst in absence of substrate. For doing that, we performed experiments under identical conditions without taking any substrate (Table 1, entry 8), and after 8 h substrate (benzaldehyde) was added. We could find only 5% conversion of benzaldehyde after 8 h reaction time instead of 86% (Table 1, entries 2 and 8). We could conjecture that this clearly indicates the first route (direct hydride transfer) as the operative mechanism here, as otherwise formate ion decomposition is not possible without the presence of substrate. Additionally, we have also performed the transfer hydrogenation of benzaldehyde in deuterated water (D₂O) as solvent with formate (HCOOK) as possible hydride source and Au-P1 catalyst. The obtained product (benzyl alcohol) was isolated, and we recorded its proton NMR spectra (Fig. S8). We could observe only hydrogen (-H) but no deuterium (-D) in the methylene peak of the product, i.e., benzyl alcohol. The observation clearly indicates that during reduction of carbonyl group, the source of proton is formate salt (-HCOOK), not water (H₂O).

Conclusions

In summary, a new type of ligand (1,4-Diethynylbenzene) stabilized gold nanoparticles mimicking graphene supported gold nanocatalyst was synthesized through a biphasic ligand exchange protocol. Monodispersed gold nanoparticles with average size of 1.8 ± 0.3 nm stabilized by polyacetylene 3D framework showed high stability against thermal and photoirradiation conditions. FT-IR analysis suggests that acetylenic protons from $-C\equiv C-H$ bonds breaks down and Au-C bond is formed where Au NPs are electronically conjugated with the polymeric

acetylene framework. The synthesized Au NPs showed high photocatalytic activity for the degradation of a range of toxic dyes in aqueous phase under visible light irradiation by using hydrogen peroxide as oxidant. The catalyst can be reused several times without any significant decrease of the catalytic activity. The possible mechanism involves dye adsorption on ligand surface followed by transfer of electron from excited dye molecule to gold via ligand conjugation. The excited electrons from Au Fermi level generate reactive hydroxyl radical ($\cdot OH$) which is responsible for breaking down the dye molecules. The catalyst also shows good efficiency for transfer hydrogenation of organic carbonyl and nitro derivatives with ease of catalyst separation for recycling and efficient reusing capacity. The preliminary mechanistic study indicates that formate ions form gold-hydride (Au-H) intermediate species.

Supplementary Information The online version contains supplementary material available at <https://doi.org/10.1007/s11051-021-05182-9>.

Funding P. M. thanks CSIR (India) (Project no. 01(2873)/17/EMR-II) for financial support, DST-FIST (India) grant for institutes (SR/FST/LSI-642/2015) is gratefully acknowledged.

Declarations

Conflict of interest The authors declare no competing interest.

References

- Akpan UG, Hameed BH (2009) Parameters affecting the photocatalytic degradation of dyes using TiO₂-based photocatalysts: a review. *J Hazard Mater* 170:520–529. <https://doi.org/10.1016/j.jhazmat.2009.05.039>
- Arabatzi IM, Stergiopoulos T, Andreeva D, Kitova S, Neophytides SG, Falaras P (2003) Characterization and photocatalytic activity of Au/TiO₂ thin films for azo-dye degradation. *J Catal* 220:127–135. [https://doi.org/10.1016/S0021-9517\(03\)00241-0](https://doi.org/10.1016/S0021-9517(03)00241-0)
- Bhowmik T, Kundu MK, Barman S (2015) Ultra small gold nanoparticles–graphitic carbon nitride composite: an efficient catalyst for ultrafast reduction of 4-nitrophenol and removal of organic dyes from water. *RSC Adv* 5:38760–38773. <https://doi.org/10.1039/C5RA04913J>
- Chavda N, Trivedi A, Thakarda J, Agrawal YK, Maity P (2016) Size specific activity of polymer stabilized gold nanoparticles

- for transfer hydrogenation catalysis. *Catal Lett* 146:1331–1339. <https://doi.org/10.1007/s10562-016-1760-3>
- Cheng N, Tian J, Liu Q, Ge C, Qusti AH, Asiri AM, Al-Youbi AO, Sun X (2013) Au-nanoparticle-loaded graphitic carbon nitride nanosheets: green photocatalytic synthesis and application toward the degradation of organic pollutants. *ACS Appl Mater Interfaces* 5:6815–6819. <https://doi.org/10.1021/am401802r>
- Choudhary BC, Paul D, Gupta T, Tetgure SR, Garole VJ, Borse AU, Garole DJ (2017) Photocatalytic reduction of organic pollutant under visible light by green route synthesized gold nanoparticles. *J Environ Sci* 55:236–246. <https://doi.org/10.1016/j.jes.2016.05.044>
- Corma A, Serna P (2006) Chemoselective hydrogenation of nitro compounds with gold catalysts. *Science* 313:332–334. <https://doi.org/10.1126/science.1128383>
- Dave P, Agrawal B, Thakarda J, Bhowmik S, Maity P (2019) An organometallic ruthenium nanocluster with conjugated aromatic ligand skeleton for explosive sensing. *J Chem Sci* 131: 14. <https://doi.org/10.1007/s12039-018-1589-y>
- Depuccio DP, Botella P, O'Rourke B, Landry CC (2015) Degradation of methylene blue using porous WO₃, SiO₂–WO₃, and their Au-loaded analogs: adsorption and photocatalytic studies. *ACS Appl Mater Interfaces* 7:1987–1996. <https://doi.org/10.1021/am507806a>
- Gilkey MJ, Xu B (2016) Heterogeneous catalytic transfer hydrogenation as an effective pathway in biomass upgrading. *ACS Catal* 6:1420–1436. <https://doi.org/10.1021/acscatal.5b02171>
- Gupta N, Singh HP, Sharma RK (2010) Single-pot synthesis: plant mediated gold nanoparticles catalyzed reduction of methylene blue in presence of stannous chloride. *Colloids Surf A Physicochem Eng Asp* 367:102–107. <https://doi.org/10.1016/j.colsurfa.2010.06.022>
- He L, Ni J, Wang LC, Yu FJ, Cao Y, He HY, Fan KN (2009) Aqueous room-temperature gold-catalyzed chemoselective transfer hydrogenation of aldehydes. *Chem Eur J* 15: 11833–11836. <https://doi.org/10.1002/chem.200901261>
- He L, Lou XB, Ni J, Liu YM, Cao Y, He HY, Fan KN (2010) Efficient and clean gold-catalyzed one-pot selective N-alkylation of amines with alcohols. *Chem Eur J* 16:13965–13969. <https://doi.org/10.1002/chem.201001848>
- Hussain M, Sun H, Karim S, Nisar A, Khan M, Haq A, Iqbal M, Ahmad M (2016) Noble metal nanoparticle-functionalized ZnO nanoflowers for photocatalytic degradation of RhB dye and electrochemical sensing of hydrogen peroxide. *J Nanopart Res* 18:95. <https://doi.org/10.1007/s11051-016-3397-y>
- Hutchings GJ, Haruta M (2005) A golden age of catalysis: a perspective. *Appl Catal A Gen* 291:2–5. <https://doi.org/10.1016/j.apcata.2005.05.044>
- Indra A, Maity P, Bhaduri S, Lahiri GK (2013) Chemoselective hydrogenation and transfer hydrogenation of olefins and carbonyls with the cluster-derived ruthenium nanocatalyst in water. *ChemCatChem* 5:322–330. <https://doi.org/10.1002/cctc.201200448>
- Lellis B, Fávaro-Polonio CZ, Pamphile JA, Polonio JC (2019) Effects of textile dyes on health and the environment and bioremediation potential of living organisms. *Biotechnol Res Innov* 3:275–290. <https://doi.org/10.1016/j.biori.2019.09.001>
- Leppelt R, Schumacher B, Plzak V, Kinne M, Behm RJ (2006) Kinetics and mechanism of the low-temperature water–gas shift reaction on Au/CeO₂ catalysts in an idealized reaction atmosphere. *J Catal* 244:137–152. <https://doi.org/10.1016/j.jcat.2006.08.020>
- Lu W, Ning R, Qin X, Zhang Y, Chang G, Liu S, Luo Y, Sun X (2011) Synthesis of Au nanoparticles decorated graphene oxide nanosheets: noncovalent functionalization by TWEEN 20 in situ reduction of aqueous chloroaurate ions for hydrazine detection and catalytic reduction of 4-nitrophenol. *J Hazard Mater* 197:320–326. <https://doi.org/10.1016/j.jhazmat.2011.09.092>
- Maity P, Tsunoyama H, Yamauchi M, Xie S, Tsukuda T (2011) Organogold clusters protected by phenylacetylene. *J Am Chem Soc* 133:20123–20125. <https://doi.org/10.1021/ja209236n>
- Maity P, Wakabayashi T, Ichikuni N, Tsunoyama H, Xie S, Yamauchi M, Tsukuda T (2012) Selective synthesis of organogold magic clusters Au₅₄(C≡CPh)₂₆. *Chem Commun* 48:6085–6087. <https://doi.org/10.1039/C2CC18153C>
- Maity P, Takano S, Yamazoe S, Wakabayashi T, Tsukuda T (2013) Binding motif of terminal alkynes on gold clusters. *J Am Chem Soc* 135:9450–9456. <https://doi.org/10.1021/ja401798z>
- Mishra A, Mehta A, Basu S (2018) Clay supported TiO₂ nanoparticles for photocatalytic degradation of environmental pollutants: a review. *J Environ Chem Eng* 6:6088–6107. <https://doi.org/10.1016/j.jece.2018.09.029>
- Ni J, He L, Liu YM, Cao Y, He HY, Fan KN (2011) Mild and efficient CO-mediated eliminative deoxygenation of epoxides catalyzed by supported gold nanoparticles. *Chem Commun* 47:812–814. <https://doi.org/10.1039/C0CC02783A>
- Noyori R, Hashiguchi S (1997) Asymmetric transfer hydrogenation catalyzed by chiral ruthenium complexes. *Acc Chem Res* 30:97–102. <https://doi.org/10.1021/ar950234i>
- Ren R, Li S, Li J, Ma J, Kiu H, Ma J (2015) Enhanced catalytic activity of Au nanoparticles self-assembled on thiophenol functionalized graphene. *Catal Sci Technol* 5:2149–2156. <https://doi.org/10.1039/C4CY01620C>
- Saqib M, Halder A (2018) Reduced graphene oxide supported gold nanoparticles for electrocatalytic reduction of carbon dioxide. *J Nanopart Res* 20:46. <https://doi.org/10.1007/s11051-018-4146-1>
- Sarina S, Waclawik ER, Zhu H (2013) Photocatalysis on supported gold and silver nanoparticles under ultraviolet and visible light irradiation. *Green Chem* 15:1814–1833. <https://doi.org/10.1039/C3GC40450A>
- Srivastav AK, Agrawal B, Swami B, Agrawal YK, Maity P (2017) Ligand exchange synthesis of organometallic Rh nanoparticles and application in explosive sensing. *J Nanopart Res* 19: 216. <https://doi.org/10.1007/s11051-017-3910-y>
- Su FZ, Liu YM, Ni J, Cao Y, He HY, Fan KN (2008) Efficient and chemoselective reduction of carbonyl compounds with supported gold catalysts under transfer hydrogenation conditions. *Chem Commun*:3531–3533. <https://doi.org/10.1039/B807608A>
- Sun X, Dong S, Wang E (2004) Large-scale synthesis of micrometer-scale single-crystalline Au plates of nanometer thickness by a wet-chemical route. *Angew Chem Int Ed* 43: 6360–6363. <https://doi.org/10.1002/anie.200461013>

- Trivedi A, Thakarda J, Chavda N, Agrawal YK, Maity P (2016) A new route towards selective synthesis of supported Cu₂O and CuO nanoparticles under extremely mild condition. *Nano-Struct Nano-Objects* 6:34–38. <https://doi.org/10.1016/j.nanos.2016.03.004>
- Tsukuda T, Tsunoyama H, Sakurai H (2011) Aerobic oxidations catalyzed by colloidal nanogold. *Chem Asian J* 6:736–748. <https://doi.org/10.1002/asia.201000611>
- Tsunoyama H, Sakurai H, Ichikuni N, Negishi Y, Tsukuda T (2004) Colloidal gold nanoparticles as catalyst for carbon–carbon bond formation: application to aerobic homocoupling of phenylboronic acid in water. *Langmuir* 20:11293–11296. <https://doi.org/10.1021/la0478189>
- Wang D, Astruc D (2015) The golden age of transfer hydrogenation. *Chem Rev* 115:6621–6686. <https://doi.org/10.1021/acs.chemrev.5b00203>
- Wang D, Han D, Yang J, Wang J, Li X, Song H (2018) Controlled preparation of superparamagnetic Fe₃O₄@SiO₂@ZnO-Au core-shell photocatalyst with superior activity: RhB degradation and working mechanism. *Powder Technol* 327:489–499. <https://doi.org/10.1016/j.powtec.2017.12.088>
- Xiong Z, Zhang LL, Ma J, Zhao XS (2010) Photocatalytic degradation of dyes over graphene–gold nanocomposites under visible light irradiation. *Chem Commun* 46:6099–6101. <https://doi.org/10.1039/C0CC01259A>
- Yamamoto H, Maity P, Takahata R, Yamazoe S, Koyasu K, Kurashige W, Negishi Y, Tsukuda T (2017) Monodisperse iridium clusters protected by phenylacetylene: implication for size-dependent evolution of binding sites. *J Phys Chem C* 121:10936–10941. <https://doi.org/10.1021/acs.jpcc.6b12121>
- Yamazoe S, Koyasu K, Tsukuda T (2014) Non-scalable oxidation catalysis of gold clusters. *Acc Chem Res* 47:816–824. <https://doi.org/10.1021/ar400209a>
- Zhu Y, Qian H, Drake BA, Jin R (2010) Atomically precise Au₂₅(SR)₁₈ nanoparticles as catalysts for the selective hydrogenation of alpha, beta-unsaturated ketones and aldehydes. *Angew Chem Int Ed* 49:1295–1298. <https://doi.org/10.1002/anie.200906249>

Publisher's note Springer Nature remains neutral with regard to jurisdictional claims in published maps and institutional affiliations.